Geometric modelling of INSAT-2E CCD payload and multistrip mosaicking for geocoding large areas

N. Padmanabhan*, R. Ramakrishnan and S. B. Gurjar

Space Applications Centre, Indian Space Research Organization, Jodhpur Tekra, Ahmedabad 380 015, India

The Indian National Satellite (INSAT-2E), a geostationary satellite, carries a Charged Coupled Device camera. This camera is of scanning-mirror-type with a large field-of-view of 10° × 10°. It generates three-band image data in strips of about 300 km in the north-south direction. This article describes a method of removing the distortions due to the scan imaging, and mosaicking the corrected strips to generate geocoded images of India and its environs. The method can be used to generate geocoded images of any area imaged by any satellite of the same type. The accuracy of the absolute earth location calculated by considering some ground control points, is found to be about 5 pixels, both in the N–S and E–W directions.

INSAT-2E is a geostationary satellite with two imaging instruments apart from the communication transponders. One of these is a Very High-Resolution Radiometer (VHRR) operating in three spectral bands. A wide panchromatic visible band images the earth disc and clouds with a resolution of 2 km × 2 km from the geostationary altitude of 36,000 km. A water vapour (WV) band maps the moisture patterns in the atmosphere, while a thermal infrared (TIR) takes thermal images of the earth and the cloud patterns. Both these infrared bands provide images with a spatial resolution of 8 km × 8 km.

The other instrument on-board INSAT-2E is a three-band Charge Coupled Device (CCD)-based imager. This instrument provides co-registered images of the earth in the visible (VIS, 0.62 to 0.68 μm), near infrared (NIR, 0.77 to 0.86 μm) and short wave infrared (SWIR, 1.55 to 1.69 μm) regions of the electromagnetic spectrum. The subsatellite point ground resolution of these images is 1 km × 1 km for all the three bands. The central wavelengths and bandwidths of the spectral bands as well as dynamic range and saturation radiance are so selected that the images can be used both for meteorological and earth resources remote-sensing applications. The payload has a basic telescope and scan mechanism for imaging. Two dichroic beam splitters achieve the separation of the three bands. The scan mirror is mounted on a two-axis gimballed scan mechanism system to generate a two-dimensional image by sweeping the detector array field-of-view across the earth's surface in west-east (fast-scan) and north-south (slow-scan) directions. The long axes of detector arrays are oriented in the north-south direction. The detector array contains 300 detector elements. The fast-scan line is scanned from west to east by the scan mirror in approximately one minute. At the end of the line, the mirror retraces to the west, is stepped south by 0.3955° and starts imaging the next line. Three hundred contiguous image lines are generated for each of the bands during one fast-scan line, and this is called a frame. The step down between two successive fast-scans is done such that there is an overlap of about 17 lines between the two successive frames. More details about the payload are given by Iyengar *et al.*[1].

Each frame covers a field-of-view of 10° in the west-east direction and about 0.3985° in the north-south direction. Hence, the resolution will be varying from one line to another and from one edge to another because of panoramic distortion. Besides, the earth curvature will also influence the resolution, making it variable. All these factors introduce distortions in the image acquired by the satellite. If the image has to be used for any application, all these distortions have to be removed.

Image correction

The CCD camera, flown for the first time in a geostationary satellite, provides a unique opportunity to the meteorologist for continuous monitoring of cloud-cover pictures in three spectral bands. Besides, the data from this sensor can be used for a number of agro-meteorological applications[2]. However, for the above-mentioned applications, the data transmitted must be geocoded. Geocoding is the process of removing the distortions in the image, aligning the same to true north, and projecting it onto a proper map projection with a constant resolution. Though the fast-scan axis of the camera is in the north-south direction, because of the interplay of the scan mechanism and the earth curvature, the frames are not truly north-aligned – there is a skew in the data, which needs to be corrected. Besides, there could be distortions due to satellite attitude.

The CCD camera images the earth surface by scanning from west to east (fast-scan), followed by a step down (slow-scan) and reverse sweep in non-imaging mode. This is followed by the next fast-scan. The data captured during each fast-scan are transmitted as a frame. In one

*For correspondence. (e-mail: sacpaddy@ipdpg.gov.in)

full acquisition, there are twenty-five such frames. Each of these frames consists of 300 lines × 7165 pixels on the ground. The raw data will have some peculiarities arising out of the non-uniform response of the different detectors in the array or due to some pixel dropouts. These are corrected in a process called radiometric correction, where the laboratory-measured response of each of the detectors is used to normalize the detector behaviour. Two successive radiometrically-corrected frames of 300 scans × 7165 pixels are shown in Figure 1. However, if we are to use the data for any application, it has to be corrected for all distortions and mapped onto a map projection plane with proper output resolutions. The distortions that are inherent in the image, and are to be removed are:

(i) Panaromic distortion – As mentioned earlier, the field-of-view of the sensor is 10° in the west to east direction and 0.3985° in the north south direction. Because of such a large field-of-view, the resolution of the image is not constant. At nadir, the resolution is about 875 m, and keeps increasing as we go to either side of the image. Besides, during slow-scan, each frame is stepped down by 0.3955°. Thus, in the north-south direction also, there is a variation in the resolutions as we go from one frame to another.

(ii) Distortion due to scanning mirror – The imaging mechanism in the camera is of scanning-mirror-type. This introduces a skew as we go from west to east in the fast-scan process. This skew coupled with the curvature of the earth, results in the image being lune-shaped.

Besides, the data of each frame will cover only 300 lines × 7165 pixels. Thus, each corrected frame covers only a small portion in the north-south direction. If our area of interest has a large north-south extent, then more than one frame has to be corrected. All these corrected images when mosaicked, will give the final corrected product (image). In fact, we are interested in generating the geocoded product of India. The country covers approximately 30° of latitude and 30° of longitude. This calls for a mosaic of about fifteen corrected frames.

Figure 1. Radiometrically corrected image frames 7 and 8.

Thus the steps involved in generating a geocoded product are grid generation, resampling and mosaicking.

Grid generation

The camera consists of a scan mirror that sweeps in the west to east direction over an angle of 10°. This sweep called fast-scan, is repeated twenty-five times, by changing the angle of the mirror in the north-south direction. The data collected during each of the fast-scans are called a frame. This way, a collection of 25 frames covers the total scene. The north-south stepping is called a slow-scan. The starting angles for both the fast-scan and the slow-scan can be set at users' request, thus enabling coverage of different areas. Grid generation is the process of establishing a mapping between the area of interest and the input frames. This mapping will be used in the further processes of resampling and mosaicking for generating the final geocoded product. The payload geometry is given in Iyengar *et al.*[1] (see Figure 5). The mathematical model used to represent the payload geometry is depicted in Figure 2.

Geometric model

The camera geometry is modelled as follows.

H_1H_2 is the detector array and OX^c is the optical axis, where O is the centre of the array. The focal point of the camera F is at a distance f from O. The mirror is represented by the plane $ABCD$, M_1M_2 and L_1L_2 being the fast and slow-scan axes respectively. These intersect at O', which is at a distance d_m from O. At rest, M_1M_2 is coplanar with and parallel to H_1H_2, while L_1L_2 makes an angle of 45° with OX^c.

The basic assumption in this model is that imaging is done by a pin-hole type of camera. The ray of light, which comes from the earth (G) strikes the mirror at P' and after reflection, goes through the focus of the system F to strike the detector P. The reflection at the mirror obeys the laws of reflection at plane surfaces and hence,

$$\angle GP'N = i = \angle NP'P = r.$$

Using the principle of reversibility of light, this means that a ray of light from a particular detector in the detector array, is reflected by the mirror and this reflected ray intersects the earth. Thus, given any pixel in the detector array, by using geometrical concepts, the position on the ground imaged by the particular detector is determined.

To do the geolocation, we have to define some coordinate systems of reference. Since the telemetry information is available in the earth centred intertial system, we first do the geolocation in this coordinate system. This is

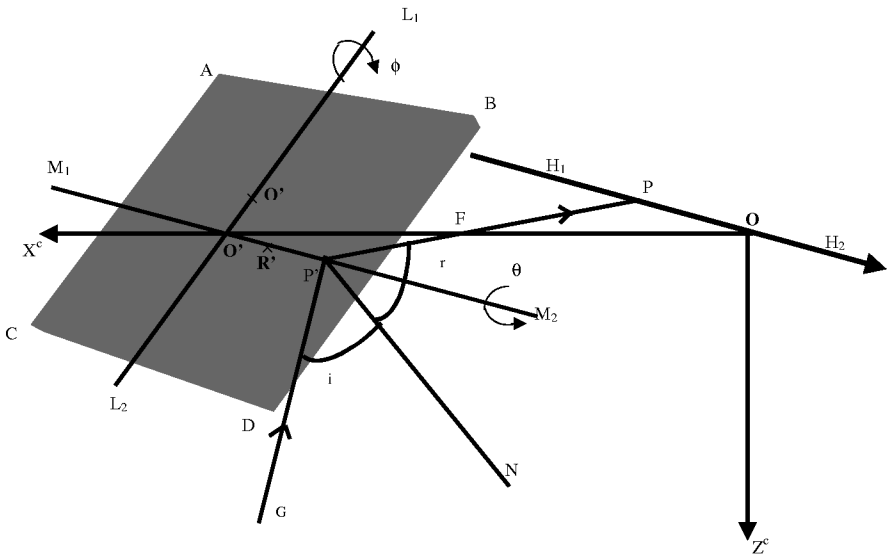

Figure 2. Schematic diagram of payload geometry. *ABCD*, Scan mirror; $OF = f$; $OO' = d_m$; L_1L_2, Slow scan axis; M_1M_2, Fast scan axis; OX^c, Principal axis; H_1H_2, Detector array with O as the central detector; ϕ, Slow scan angle, and θ, Fast scan angle.

transformed to the geographical coordinates for the final image correction. Patt and Gregg[3] have given a solution for geolocation in the sensor frame of reference.

We choose the following coordinate systems:

Camera coordinate system: In this, the origin is the middle detector, the Y^c-axis is the detector array, X^c-axis is the line perpendicular to the array through the centre detector. The Z^c-axis is chosen in such a way that they form a right-handed system of coordinates.

Orbital system of coordinates: Origin is the satellite, y^0-axis is the velocity vector (roll axis), x^0-axis is the pitch axis and z^0-axis is the nadir direction (yaw axis). Thus, the angles between the corresponding axes of these two systems of coordinates give the attitude angles.

Inertial frame of reference: Origin is the centre of the earth, z^i-axis is earth's polar axis, x^i-axis is towards vernal equinox true of date and y^i-axis is so chosen that they form a right-handed coordinate system, the x^iy^i plane being the equatorial plane.

Thus, for pixel number p, if d is the detector size, then the camera coordinates are

$$(x_p^c, y_p^c, z_p^c) = (0, (p - p_c)*d, 0). \quad (1)$$

If the focal length is f, then the coordinates of the focus are

$$(x_f^c, y_f^c, z_f^c) = (f, 0, 0). \quad (2)$$

Here (x_p^c, y_p^c, z_p^c) refers to the coordinates of the pixel under consideration in the camera coordinate system and p_c is the detector number through which the principal axis (OO') passes. In our case, p_c is the middle detector and hence is 150, since the total number of elements in the array is 300.

The mirror is assumed to be a plane. In the resting state, the mirror makes an angle of 45° with the plane determined by M_1M_2 and H_1H_2 and the north-south angle is 0°. To find the coordinates of the point P', we have to solve the equations representing the line PF and the equation representing this mirror. To do this, we shall first find out the direction cosines of the mirror plane. Let the fast and slow angles at any instant of time be θ and ϕ respectively. We consider three points on the mirror – O', the point of intersection of the X^c-axis with the mirror; R', a point on the mirror's rotation axis at a unit distance, and Q', a point at a unit distance perpendicular to this line.

The coordinates of these three points are thus O' (x_1^c, y_1^c, z_1^c), R' (x_2^c, y_2^c, z_2^c) and Q' (x_3^c, y_3^c, z_3^c). Since these three points are non-collinear, and their coordinates are known, the equation to the mirror plane can be established. The direction ratios of the lines $Q'R'$, $O'Q'$ and $O'R'$ are

$$\begin{aligned} &\text{vect}_1x = x_2^c - x_3^c,\ \text{vect}_1y = y_2^c - y_3^c,\ \text{vect}_1z = z_2^c - z_3^c \\ &\text{vect}_2x = x_1^c - x_3^c,\ \text{vect}_2y = y_1^c - y_3^c,\ \text{vect}_2z = z_1^c - z_3^c \\ &\text{vect}_3x = x_1^c - x_2^c,\ \text{vect}_3y = y_1^c - y_2^c,\ \text{vect}_3z = z_1^c - z_2^c. \end{aligned} \quad (3)$$

The direction cosines of these three lines can then be determined by normalizing these direction ratios. The coordinates of the three points mentioned above are dependent on the fast-scan angle and the slow-scan angle.

The direction cosines of the normal to the mirror in the camera coordinate system are obtained as

$$L^{c}_{nor} = \text{vect}_1 y * \text{vect}_2 z - \text{vect}_1 z * \text{vect}_2 y$$
$$M^{c}_{nor} = \text{vect}_1 z * \text{vect}_2 x - \text{vect}_1 x * \text{vect}_2 z \quad (4)$$
$$N^{c}_{nor} = \text{vect}_1 x * \text{vect}_2 y - \text{vect}_1 y * \text{vect}_2 x.$$

Again normalizing these direction ratios, we can obtain the direction cosines of the normal to the mirror plane. Since the mirror plane passes through the points $(x^{c}_1, y^{c}_1, z^{c}_1)$, and the direction cosines of the normal are known, the equation to the mirror plane can be written in the form

$$ax + by + cz + d = 0. \quad (5)$$

a, b, c, d are constants representing the mirror plane. These depend on the direction cosines of the normal to the mirror as given in eq. (4) above.

Now, the equation to line PF is given by

$$(x - x^{c}_1)/(x^{c}_2 - x^{c}_1) = (y - y^{c}_1)/(y^{c}_2 - y^{c}_1) = (z - z^{c}_1)/(z^{c}_2 - z^{c}_1). \quad (6)$$

This line intersects the mirror at P'. Solving the equations to the line and the mirror, we get the coordinates of the point P' $(x^{c}_q, y^{c}_q, z^{c}_q)$.

The ray of light that comes from the detector P strikes the mirror at P' and gets reflected. The direction cosines of the reflected ray are found out using the laws of reflection:

(i) The reflected ray, incident ray and the normal should be in the same plane;
(ii) The angle of incidence and the angle of reflection should be equal.

Let the direction cosines of the reflected ray be $(l^{c}_{ref}, m^{c}_{ref}, n^{c}_{ref})$ in the camera coordinate system. Using the different coordinate systems defined earlier, these direction cosines and the coordinates of the P' can be transformed first to the orbital system of coordinates and then to the inertial system of coordinates by simple matrix multiplications. Let them be $(l^{i}_{ref}, m^{i}_{ref}, n^{i}_{ref})$ and $(x^{i}_q, y^{i}_q, z^{i}_q)$. We can now get the equations to the reflected ray in the inertial system of reference.

Earth is a complicated three-dimensional surface, and hence modelling it accurately is quite complicated. However, depending on the area of study, the earth is modelled by ellipsoids with suitable semi-major and semi-minor axes, so that the approximation is close to the area of interest.

Thus, let the earth be represented by the ellipsoid

$$x^2/a^2_e + y^2/b^2_e + z^2/c^2_e = 1 \quad (7)$$

in the inertial system of coordinates. Here, a_e, b_e and c_e are the parameters of the ellipsoid, and are known. Since the earth is in reality a spheroid, a_e and b_e are taken equal. For Indian regions, the ellipsoid parameters are 6378, 6378 and 6356 km. The equations to the reflected ray and the ellipsoid are solved to obtain the coordinates of the point imaged on the ground (surface of the earth). While solving equations (6) and (7), sometimes, the equations might not have any solution, indicating no intersection. This corresponds to the case when the camera is looking into cold space. Such singular situations are handled by introducing fictitious values for the point of intersection.

Verification of the mathematical model

To validate this model, an analysis was done as follows. The earth is considered to be a simplistic plane below the satellite at a distance of 36,000 km. Varying the slow-scan angle and the fast-scan angle, we found the coordinates of the points imaged by the two extreme detector elements of the detector array. The results of this analysis are given in Table 1.

In Table 1, ϕ corresponds to slow-scan angle in degrees, while θ corresponds to fast-scan angle in degrees. The model was used to find the ground coordinates for pixel numbers 1 and 300. Let their coordinates be ($x\text{ground}_1$, $y\text{ground}_1$, $z\text{ground}_1$) and ($x\text{ground}_2$, $y\text{ground}_2$, $z\text{ground}_2$) and

$$\delta x = (x\text{ground}_1 - x\text{ground}_2),$$

$$\delta y = (y\text{ground}_1 - y\text{ground}_2).$$

Dividing δy by the number of detectors, which is 300, we obtain the ground resolution given in the last column. δx gives the difference in the position on the ground of the features imaged by the first and last detectors. Thus, this gives the skew in the ground features imaged by the detector as it scans from west to east and north to south. We

Table 1. Skew in the various frames of INSAT-2E CCD payload. Earth is taken as a plane at 36,000 km below the satellite

ϕ (degrees)	θ (degrees)	δx (m)	δy (m)	Resolution (m)
−4.5	40	−25207	267595	892
−4.5	45	−20778	263190	877
−4.5	50	−17670	267007	890
−5.0	40	−28078	267873	892
−5.0	45	−23132	263383	877
−5.0	50	−19663	267146	890
0.0	40	0	266419	888
0.0	45	0	262372	875
0.0	50	0	266419	888
5.0	40	28078	267872	893
5.0	45	23131	263388	878
5.0	50	19663	267145	890

observe from Table 1, that as we go from west to east along a frame, the skew angle varies. Moreover, it also varies from one frame to another.

It can be seen that for slow-scan angle zero, i.e. when the satellite is imaging vertically down, there is no skew observed. In other words, for the slow-scan position which corresponds to the nadir look, as the mirror moves in fast-scan mode, the imaged lines are all exactly parallel to the north-south direction. However, when the slow-scan angle is non-zero, there is skew in these imaged lines. It can further be observed, that as the slow-scan angle changes sign, i.e. imaging is done on two different sides of the nadir, the skew also changes direction. If the earth is modelled as a spheroid, then this mapping will be more complicated.

Geometric correction algorithm

The geometric model developed above is incorporated in the geometric correction algorithm.

Image to ground mapping: The first step is to find the coordinates of the points imaged by the various detector elements during the full slow/fast-scan. The slow-scan and fast-scan angles are obtained from the telemetry data coming along with the video data. The satellite state vector is obtained using an orbit determination algorithm. Since the satellite is geostationary and the field-of-view is 10° in both north-south and west-east directions, sometimes, the satellite might look into cold space. This is taken care in the model.

In one frame, the slow-scan angle varies from say ϕ_{st} to ϕ_{end}, while the fast-scan angle varies from θ_{st} to θ_{end}.

For

$$\phi_{st} \le \phi \le \phi_{end},\ \theta_{st} \le \theta \le \theta_{end},$$

using the geometric model described in the previous section and modelling the earth as a spheroid, the point on the ground imaged by a particular detector element is found out as (x_g^i, y_g^i, z_g^i) in the inertial frame of reference.

The geocentric latitude is obtained as

$$\varphi_c = \tan^{-1}\left(z_g^i / \sqrt{(x_g^{i2} + y_g^{i2})}\right)$$

and geocentric longitude is obtained as

$$\chi = \tan^{-1}(y_g^i / x_g^i). \quad (8)$$

Using the time of imaging, the sidereal angle (SA) is calculated and the geodetic longitude is then obtained as

$$\lambda = \chi - \mathrm{SA}.$$

The geodetic latitude is obtained as

$$\varphi = \tan^{-1}\left(b_e^2 / a_e^2 \tan \varphi_c\right),$$

where a_e and b_e are the parameters of the spheroid representing the earth.

Thus, the mapping

$$(\text{detector\_no}, \theta, \phi) \rightarrow (\varphi, \lambda) \quad (9)$$

is established.

Here ϕ corresponds to the slow-scan angle and thus the different frames, while θ corresponds to the fast-scan angle. In terms of the data received on the ground, which for a frame consists of 7165 pixels × 300 lines, this mapping is equivalent to

$$(p, s) \rightarrow (\varphi, \lambda) \text{ for each frame.}$$

Here p and s stand for pixel and scanline in the image data of each frame with $1 \le p \le 7165$ and $1 \le s \le 300$. These are converted to map-projection coordinates, easting and northing[4]. Thus, the input to map-projection coordinate system map is

$$f: (p^{in}, s^{in}) \rightarrow (E^{in}, N^{in}) \text{ for each frame.}$$

Let these mappings be called I_n, $n = 1, \ldots, 25$.

Since doing this kind of mapping for each pixel is computationally tedious, the mapping is done at discrete intervals. It is observed from the mapping that in every line, the latitude decreases from the western extremity, reaching a minimum at the centre, and then increases towards further east, as shown in Figure 3. Thus, the input-to-output mapping has a lune shape. This is due to the combined effect of the imaging geometry and the spheroidal nature of the earth.

Ground-to-image mapping: The aim of the software is to generate a geocoded product of India and its surroundings (or any area of interest). The corner coordinates (φ_i, λ_i), $i = 1, 2, 3, 4$ are given a priori, where $\varphi_1 = \varphi_2$, $\varphi_3 = \varphi_4$, and $\lambda_1 = \lambda_3$, $\lambda_2 = \lambda_4$. These are converted into map-projection coordinates (E_i^{out}, N_i^{out}), $i = 1, 2, 3, 4$ using the same parameters as for the input mapping.

Let N_1 and N_2 be the minimum and maximum of N_i^{out}, and let E_1 and E_2 be the minimum and maximum of E_i^{out} for $i = 1, 2, 3, 4$.

This defines the output space as

$$N_1 \le N \le N_2$$

$$E_1 \le E \le E_2.$$

Using the output resolution, the number of lines and pixels in the output space is computed.

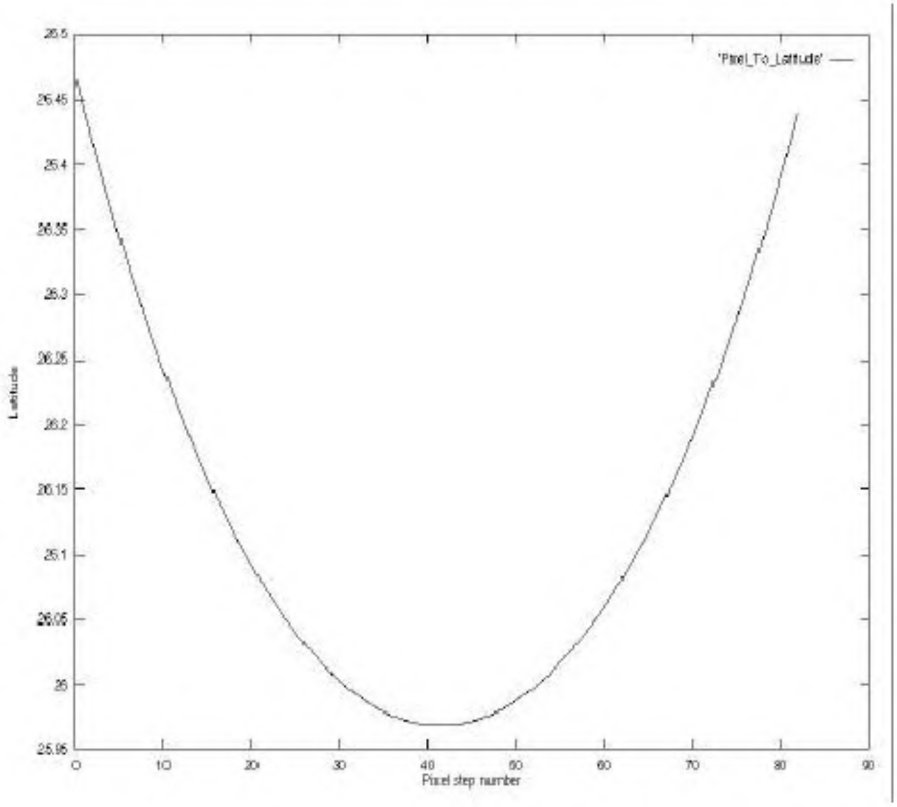

Figure 3. Plot of input-to-output mapping at step size of 80 pixels for a line. Latitude in degrees.

We have already obtained a mapping from image to map-projection coordinates for each frame. The area of interest is also available in map-projection coordinates. Since the area of interest is much larger than the area imaged by one frame, to generate a product, the area of interest has to be mapped onto the input space of each frame and then mosaicked. This is accomplished by doing a reverse mapping from the area of interest to the input space of each frame.

For this, two sets O and I_n are used, and using a simple search algorithm on the map-projection coordinates, the corresponding input pixel/scanline is obtained. This way, we establish an output-to-input mapping of the form

$$f: O \to I_n$$

$$(x_0, y_0) \to (p_{\text{in}}^{\text{n}}, s_{\text{in}}^{\text{n}}) \tag{10}$$

corresponding to each of the input frames. Thus, there is a natural partition of the output space into a number of output frames. To avoid computational load, this mapping is not done for each pixel of the output space. The output space O is divided into primary grid points $(P_i^{\text{out}}, L_i^{\text{out}})$ of size 64 lines × 64 pixels. Mapping will be done only for these primary grid points. The four neighbouring primary grid points, $(P_i^{\text{out}}, L_i^{\text{out}})$, $(P_i^{\text{out}}, L_{i+1}^{\text{out}})$, $(P_{i+1}^{\text{out}}, L_i^{\text{out}})$ and $(P_{i+1}^{\text{out}}, L_{i+1}^{\text{out}})$ are said to form a primary grid block. The resampling process will consider these primary blocks and generate corrected data in each of the blocks.

The input-to-output mapping as mentioned earlier is not a rectangle. However, the output space as defined above is a rectangle, with all points in one line having the same latitude. Hence, while doing a reverse mapping from the output space to the input space, some of the points in the output space will not have any corresponding point in the input space. To overcome this problem, we consider the input space to contain 700 lines instead of the actual 300 lines, i.e. we extend the array by 200 detectors on either side. Thus, the lune-shaped input space is enlarged. This ensures that for every point in the rectangular output space, there is a point in the enlarged lune-shaped input space.

Using the output-to-input mapping, we generated resampled images of the different output frames. The zeroes in the resampled images correspond to the extended portion of the input space. The common features in the successive resampled frames should be in the same pixel location, so that a simple joining of these resampled frames will give the complete geocoded product. However, we observe that the common features in successive resampled frames are not located at the same pixel location. This variation in the location of the common feature depend on the instrument characteristics. In the data considered for this analysis, this variation was at most 4 pixels. This in-

dicates that the grid mappings developed so far using instrument knowledge need to be fine-tuned using the image information.

Updating the grid: According to the payload specifications, two successive image frames should have an overlap of about 17 scanlines. This fact is utilized in updating the grid generated. We consider about 100 points P_i^{out} at intervals of 60 pixels along the lower edge of the output frame n. These should correspond to 100 points $P_i'^{\text{out}}$ along the upper edge of the output frame $n + 1$. By the geometrical model developed so far, these should correspond to P_i^{in} and $P_i'^{\text{in}}$. We select a window area W_i around P_i^{in} and a search area S_i around $P_i'^{\text{in}}$. These are chosen in such a way that both the window and the search area lie entirely within the respective frames. Using a correlation technique, the exact match between W_i and S_i is found. Although correlation is a rugged technique, it has some drawbacks, particularly when the scenes are cloudy, or when the radiometry of the two areas varies drastically. In such cases, we might get false correlations. These are eliminated by statistical considerations. Thus, we get the actual mapping of a pixel in the nth frame to the corresponding pixel in the $(n + 1)$th frame. At these points, the correspondence established by the geometric model described earlier is also available. These two mappings for the same pixel give the bias in the geometrical model.

Using the estimated bias in scanlines and pixels between the mapping of frame n and frame $n + 1$, the grid of frame $n + 1$ is updated. This modified grid of frame $n + 1$ will have a one-to-one mapping at the common portion with the grid of frame n. This mapping is such that the common features in two successive frames will be mapped to the location actually found in the radiometric image. Having modified frame $n + 1$ with respect to n, frame $n + 2$ is modified with respect to frame $n + 1$. This process of updating the grid is carried out from the first to the last of the relevant frames. These grids are the final ones to be used for resampling. Resampled images of successive frames using updated grids are observed to have the same feature at the same pixel location.

Resampling

The updated grids obtained above are used for resampling each of the output frames. Resampling can be done using any of the standard kernels[5]. Since the data are of 10 bits, we have used the cubic convolution kernel. Resampling is done blockwise corresponding to each primary grid block. These resampled blocks, which will be of size 64 pixels × 64 lines, are combined to generate 64 lines of output image. This process is repeated to generate the resampled image of the entire output frame. To take care of the peculiar input-to-output mapping, grid mapping is obtained for 200 extra detectors on either side of the detector array. Since these extra detectors are virtual, the mapping for these extra detectors is also virtual, and hence the resampled image contains zeroes corresponding to these virtual detectors at the top and bottom, as shown Figure 4. This is the reason for the lune shape of the video data in the resampled images.

Mosaicking

Mosaicking of all the resampled frames is done two at a time. Consider frames O_n and O_{n+1}. Since $O_n \cap O_{n+1} \neq \varnothing$, there are lines common to these resampled images. Let L be the primary grid line in O_n, which corresponds to the first primary grid line of O_{n+1} (these can be identified by their northing values). Beyond L to the end of frame O_n, the curved structure of the video data gives the following characteristics to the common data of O_n and O_{n+1}:

(a) The pixel has zero value in O_{n+1} but non-zero in O_n;
(b) The pixel has zero value in O_n but non-zero in O_{n+1};
(c) The pixel has non-zero value in both O_n and O_{n+1};
(d) The pixel has zero value in both O_n and O_{n+1}.

Mosaicking of data from O_n and O_{n+1} is done according to the following rules. From the first line to L of O_n, data are written as such onto the output image T. From L to the end

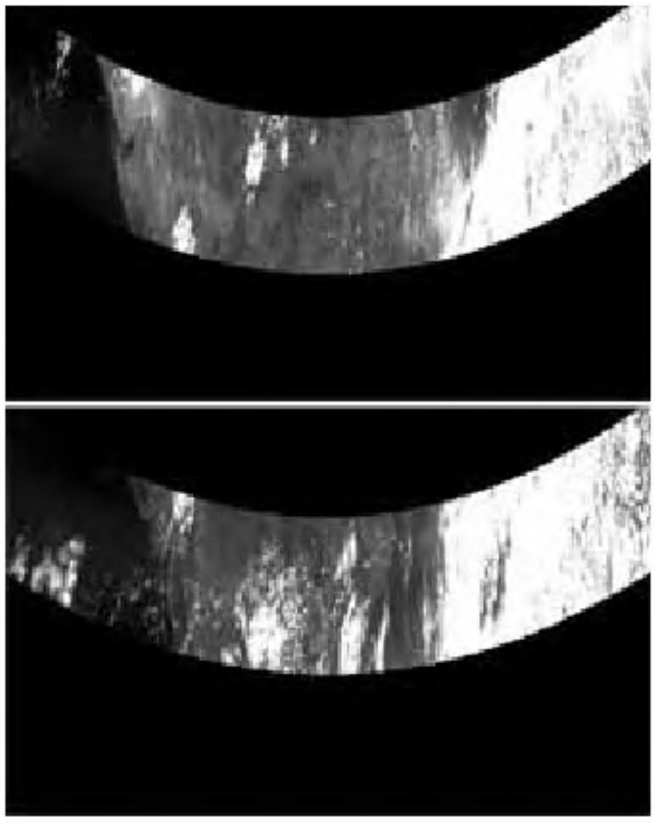

Figure 4. Resampled images of frames 7 and 8.

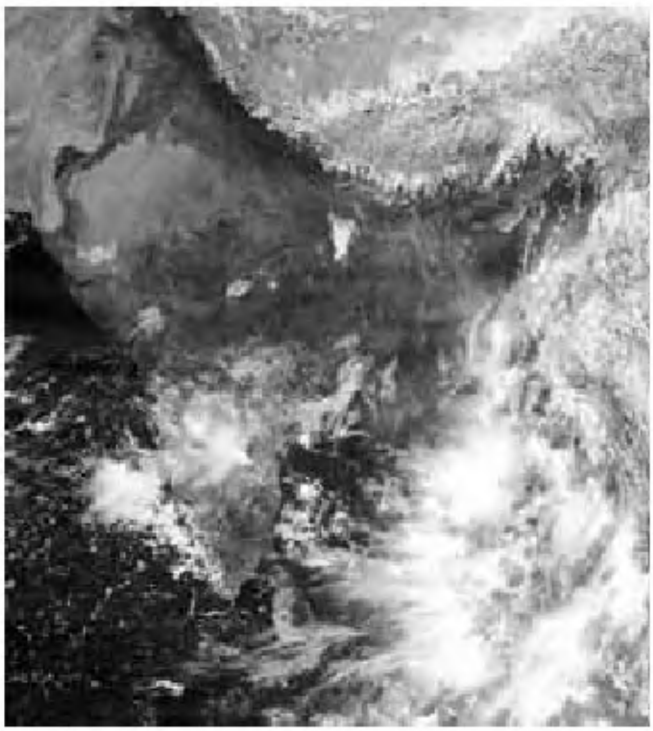

Figure 5. Final product.

of O_n, since the data are available in O_{n+1} also, the grey value assigned is obtained from O_n or O_{n+1}, whichever is non-zero, however, if both are zero, the grey value zero is assigned to the corresponding pixel in T, while if both are non-zero. Data from O_{n+1} are assigned. After the end of O_n, the data from the relevant portion of O_{n+1} are copied as such. This process is continued until all the relevant output frames are mosaicked. The output is shown in Figure 5.

Results and discussion

The above-mentioned technique was applied on the INSAT-2E CCD data of several dates and FCC products were generated. The results given above correspond to the data of 13 October 1999. After the grids were generated, the individual frames were resampled using the method mentioned earlier. Two of the resampled frames are given in Figure 4. The video data in the resampled images take a lune shape because of the combined effect of the imaging geometry and the spheroidal nature of the earth, as explained earlier. It is observed that in these two resampled frames, the same features lie at the same pixel position, thus enabling mosaicking.

Using the technique mentioned above, the final product, which is generated by mosaicking fifteen frames, is shown in Figure 5 (one band). It is observed that the mosaicking is done well and there is no feature that is repeated or cut in the overlap portions.

The methodology has been applied on a number of other datasets, including the data having cloud cover, and was found to work satisfactorily. This is because the input data cover such a large portion of the earth, that at no point of time is an entire input frame completely covered with cloud. In fact, even during the peak monsoon period of the Indian subcontinent, the method mentioned is found to work well.

Though we have generated products covering only the Indian subcontinent, there is no restriction on the method for generating products corresponding to other regions that are imaged by the satellite. In fact, the advantage of this method is that it can be used to generate geocoded products of any region imaged by the satellite. The model takes care of the panoramic distortion, earth rotation effect and attitude effect, and generates a product in the desired map projection at the desired output resolution.

The model introduces an error of about one pixel. The rest of the error in the product accuracy comes from the input errors – the major source being the attitude. Since we are updating the grid mapping between successive frames using the image data, the relative uncertainty in attitudes between successive frames is eliminated, and thus the internal distortion in the image is reduced. However, the absolute location accuracy depends on the attitude of the first frame, and the orbit determination accuracy. From a height of 36,000 km (for geostationary satellites), an error of 1° in roll/pitch corresponds to 600 km in the west-east/north-south direction. For the data considered, the accuracy figure was calculated by considering some ground-control points and was found to be about 5 pixel both in north/south and west/east directions. This value is uniform throughout the image, thus indicating that the internal distortion is practically zero.

Conclusion

A method for generating corrected products of data from INSAT-2E payload is developed. This method can be used for generating corrected products from other similar payloads. In fact, the method can be used to generate geocoded products from INSAT-3A data, which will be available soon. The geolocation algorithm used is similar to that of Patt and Gregg[3]. However, we have worked in the earth-centred inertial frame of reference, unlike their work which is based on the sensor frame of reference. This method tackles the complications introduced by the interaction of the scanning mechanism and the large field-of-view leading to corrected frames in the form of circular sectors. The method also gives an insight into the approach to be adopted for large-scale mosaicking – in fact, generation of geocoded products for the Indian subcontinent involves fifteen mosaics, as mentioned earlier. The seamless mosaic generated shows that the method can be applied for other problems that call for large-scale mosaicking.